ORGANOMETALLICS

pubs.acs.org/Organometallics Article

Steric and Electronic Effects Responsible for *N,O*- or *N,N*-Chelating Coordination of Pyrazolones Containing a Pyridine Ring in Ruthenium Arene Systems

Lorenzo Pietracci, Riccardo Pettinari,* Alessia Tombesi, Fabio Marchetti, Claudio Pettinari, Agustín Galindo, Farzaneh Fadaei-Tirani, Mouna Hadiji, and Paul J. Dyson*

Cite This: *Organometallics* 2023, 42, 1495−1504 Read Online

ACCESS | Metrics & More | Article Recommendations | Supporting Information

ABSTRACT: Structural and electronic factors are crucial to rationalize the different *N,O* or *N,N* chelating coordination of pyrazolones containing a pyridine ring. The reactivity of proligand 3-phenyl-1-(pyridin-2-yl)-5-pyrazolone ($HL^{py,ph}$) with the (arene)-Ru(II) fragment was explored. Neutral and ionic (arene)Ru(II) complexes were obtained and fully characterized, also by X-ray diffraction, revealing the ligand to coordinate in an unusual *N,O*-chelating fashion. Other ruthenium complexes were also synthesized with 3-methyl-1-(pyridin-2-yl)-5-pyrazolone ($HL^{py,me}$) and 3-methyl-1-(pyridin-2-yl)-4-trifluoroacetyl-5-pyrazolone ($HQ^{py,CF3}$). In these complexes the ligands adopt the preferred *N,N*-chelating mode. Ligands and complexes were theoretically analyzed by density functional theory (DFT). The most stable tautomer of $HL^{py,ph}$ matched well with the experimental behavior of this proligand and the structures of Ru-complexes were well described by calculations. The thermodynamic stability of the *N,O*- and *N,N*-coordination modes was analyzed and a proposal for the achievement of the *N,O*-coordination mode in complexes **1**−**4** was proposed. Cytotoxicity tests were performed against human ovarian carcinoma (A2780 and Cisplatin-resistant A2780cis) and nontumorigenic human embryonic kidney (HEK293T) cell lines, showing the free ligands to be more cytotoxic that the ensuing (arene)Ru(II) complexes.

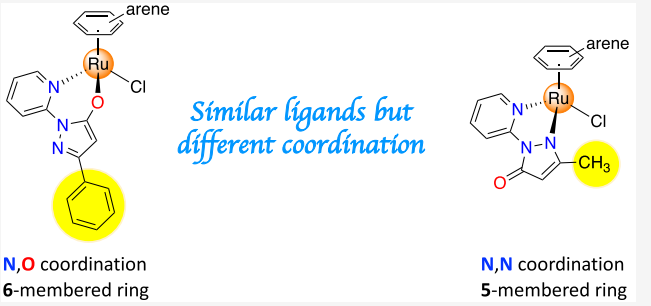

INTRODUCTION

Pyrazole is a unique five-membered heterocycle, containing two adjacent nitrogen atoms, and is considered a very important ligand in coordination chemistry because it can form a variety of coordination complexes with several metal ions, providing varying coordination geometries and nuclearities. Pyrazole and its synthetic derivatives have a broad spectrum of applications,[1,2] and in particular two classes of compounds have been intensively studied, pyrazolones and, by acylating the C-4 position, acylpyrazolones (Chart 1). Our group has contributed to this field, through the design and synthesis of numerous metal complexes using chelating acylpyrazolones and pyrazolones-based ligands.[3−5] Recently, we expanded our studies on arene-Ru(II) chemistry of two proligands, namely 3-methyl-1-(pyridin-2-yl)-5-pyrazolone ($HL^{py,me}$) and 3-methyl-1-(pyridin-2-yl)-4-trifluoroacetyl-5-pyrazolone ($HQ^{py,CF3}$, Chart 2).[6] The two ligands were found able to coordinate (in the deprotonated form) to Ru(II) in a bidentate *N,N*-fashion,[6] which is structurally analogous to some very cytotoxic Ru(II)- and Os(II)-arene phenylazopyridine complexes.[7−9]

Chart 1. Pyrazolone and Acylpyrazolone Ligands

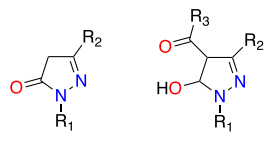

Pyrazolones (HL') Acylpyrazolones (HQ')

Chart 2. Proligands Used in This Work

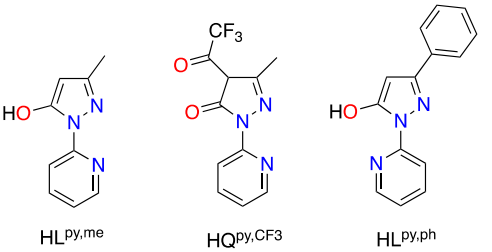

$HL^{py,me}$ $HQ^{py,CF3}$ $HL^{py,ph}$

Received: March 6, 2023
Published: May 12, 2023

Both proligands and their neutral arene-Ru(II) complexes (arene = cymene and hexamethylbenzene) were tested against A2780 and A2780cis tumor cell lines and compared to HEK293T nontumor cell lines, giving some promising results.[6] On this basis, here we expand our investigation on another pyrazolone proligand, namely 5-phenyl-2-(pyridin-2-yl)-2,4-dihydro-3*H*-pyrazol-3-one, with a phenyl replacing the methyl group in position 3 of the pyrazolone ring ($HL^{py,ph}$ in Chart 2), and to the corresponding neutral arene-ruthenium complexes.

The proligand $HL^{py,ph}$ with binding potential has been previously reported by others,[10−12] and its crystal structure solved by Watkins et al.,[13] but its coordinating ability toward metal ions is still unexplored. Moreover, we have introduced 1,3,5-triaza-7-phosphaadamantane (PTA) phosphine in the ruthenium environment by replacing the chloride ligand, affording cationic complexes with the aim to improve solubility in water.

RESULTS AND DISCUSSION

The proligand $HL^{py,ph}$ is similar to $HL^{py,me}$ (Chart 2) but with a phenyl replacing the methyl in 3-position of pyrazole. In principle, four tautomeric forms, two of which have additional rotamers, are possible for $HL^{py,ph}$ (Chart 3).

Chart 3. Possible Tautomers (I−IV) and Rotamers (I-r and IV-r) of $HL^{py,ph}$[a]

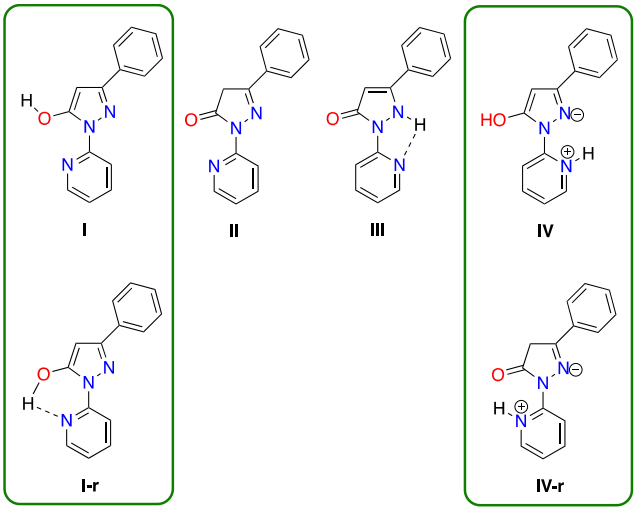

[a]Rotamer I-r is observed in the solid state and chlorinated solvents.

In the solid state the structure previously determined by X-ray crystallography[13] corresponds to rotamer I-r, which is stabilized by the intramolecular hydrogen bond O−H···N. Rotamer I-r is the only observed in chlorinated solvents, as indicated by the broad resonance at 12.86 ppm found at room temperature in the ^{1}H NMR spectrum. N−H coupling was not observed in the HSQC ^{1}H−^{15}N NMR spectrum at room temperature, providing additional evidence for the presence of enol group in $CDCl_3$. Arene-Ru(II) complexes **1** and **2** were synthesized from reaction of $HL^{py,ph}$ with $[Ru(arene)Cl_2]_2$ [where arene = p-cymene (cym) or hexamethylbenzene (hmb)] in methanol in the presence of KOH (Scheme 1). Complexes **3** and **4** were obtained by reaction of **1** and **2** in methanol with aqueous $AgBF_4$ to remove the chloride from the Ru(II) coordination sphere, followed by addition of PTA (Scheme 1).

Scheme 1. Synthesis of Complexes 1−4

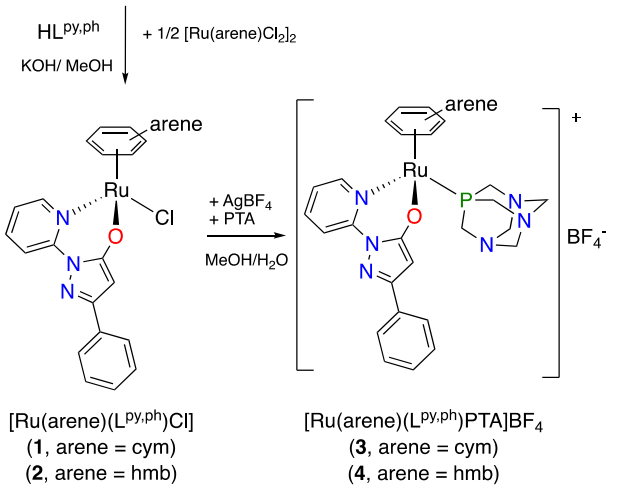

Note that in these complexes the $L^{py,ph}$ ligand acts as *N,O*-chelating donor toward the organometallic fragment (see also below in the X-ray diffraction study), whereas in previous studies the analogous $L^{py,me}$ ligand preferred to coordinate to ruthenium in a *N,N*-chelating fashion. The different behavior of the two ligands may be ascribed to the electron-withdrawing phenyl ring in $L^{py,ph}$ which depletes of electron density the N2 atom of pyrazole, causing it to coordinate through the oxygen. The ionic nature of **3** and **4** is confirmed by conductivity measurements in DMSO with Λ_m values in the range 23−26 cm^2 mol^{-1}, typical of 1:1 electrolytes.[14] The solubility in polar solvents increases from neutral **1** and **2** to ionic **3** and **4**, the latter being slightly soluble in water. ESI-MS of **1** and **2** performed in acetonitrile/methanol show main peaks due to $[Ru(arene)(L^{py,ph})]^+$ generated by the loss of the chloride ligand, whereas for **3**−**4** both $[Ru(arene)(L^{py,ph})]^+$ and $[Ru(arene)(L^{py,ph})(PTA)]^+$ species are observed. The most relevant feature in the IR spectra is the progressive decrease of the ν(C═O) vibration mode from 1654 cm^{-1} in $HL^{py,ph}$ to 1632−1635 cm^{-1} in the neutral complexes **1** and **2**, in accordance with coordination in *N,O*-chelating mode by deprotonation of tautomer I of proligand, and to 1626 and 1587 cm^{-1} in the spectra of **3** and **4** respectively, due to the positive charge of the complexes which further strengths the Ru−O bonding thus reducing the C═O bonding order.[15−18] In the IR spectra of **3** and **4** strong and sharp absorptions at ca. 1054 and 1028−1034 cm^{-1} confirm the presence of the BF_4^- anion.[19] In the far-IR region strong bands due to ν(Ru−N), ν(Ru−O), and ν(Ru−Cl) stretching modes in **1** and **2** were tentatively assigned below 500 cm^{-1}.[20] The proton and carbon assignments of the free ligand and complexes **1**−**4** have been made based on {^{1}H−^{1}H}-COSY, {^{1}H−^{13}C}-HSQC, and {^{1}H−^{13}C}-HMBC spectroscopy (Figures S6−S37).[21] The ^{1}H and ^{13}C NMR spectra of **1**−**4** recorded in $CDCl_3$ or CD_3CN show the expected shift in frequency for the resonances of the pyrazolone and pyridyl ring protons and carbon atoms in comparison to the free ligand. Moreover, in the ^{31}P NMR spectra of **3** and **4**, the phosphorus of PTA affords a singlet at −37.7 and −40.7 ppm, respectively. On the basis of the different coordination observed with $HL^{py,ph}$ ligand with respect to $HL^{py,me}$ and $HQ^{py,CF3}$, we decided to verify if these differences persisted also in their corresponding cationic complexes with PTA. The new complexes **5**−**8** were prepared using a procedure similar to that employed for **3** and **4**, starting from [Ru(arene)-

https://doi.org/10.1021/acs.organomet.3c00121
Organometallics 2023, 42, 1495−1504

($L^{py,me}$)Cl] (Scheme 2) and [Ru(arene)($Q^{py,CF3}$)Cl] (Scheme 3).[6]

Scheme 2. Synthesis of Complexes 5 and 6

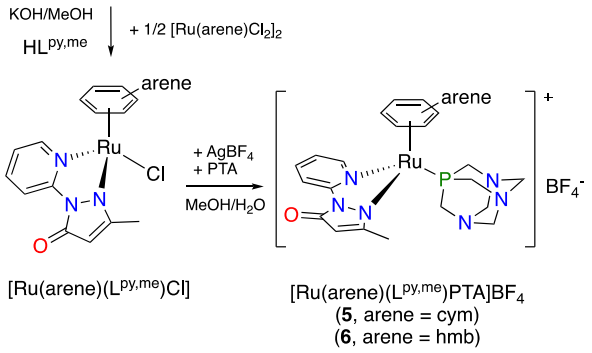

Scheme 3. Synthesis of Complexes 7 and 8

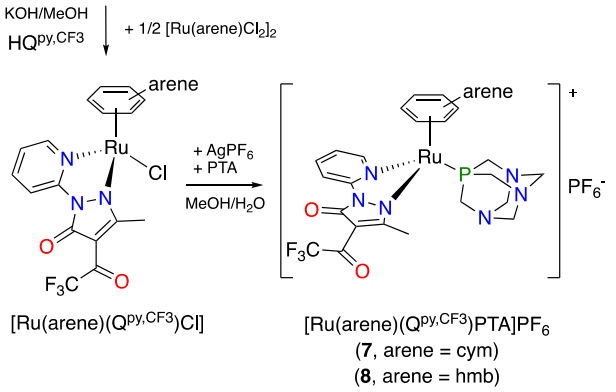

In **5**−**8** the ligands act in a *N*,*N*-chelating fashion, and in general their solubility in common solvents is lower than **1**−**4**. Complexes **5**−**8** are all 1:1 electrolytes in DMSO, in accordance with their ionic formulation. The IR spectra of **5**−**8** display a shift of the ν(C═O) to higher frequencies upon coordination, in accordance with noninvolvement of the O atom(s) of the pyrazolone moiety. The presence of BF_4^- in **5** and **6** is confirmed by the medium-to-strong bands at ca. 1050 and 1030 cm^{-1}, and a very strong absorption at 834 cm^{-1} due to PF_6^- is observed in the IR spectra of **7** and **8**.[22,23] ESI-MS of **5** and **6** display peaks due to [Ru(arene)($L^{py,me}$)]$^+$ and [Ru(arene)($L^{py,me}$)PTA]$^+$ fragments, whereas in the spectra of **7** and **8** a unique peak is observed corresponding to [Ru(arene)($Q^{py,CF3}$)PTA]$^+$. In ^{1}H and ^{13}C NMR spectra of **5**−**8** the expected change of resonances was observed for the proton and carbon atoms of the pyrazolone ligands upon coordination (Figures S38−S67). The ^{31}P NMR spectra of **7** and **8** contain a singlet at −32 and −40 ppm, respectively, with the PF_6^- anion giving a multiplet (hept) at ca. −143 ppm, due to coupling with fluorine atoms. By comparison of the {^{1}H−^{15}N}-HMBC spectra of the free ligands with their metal complexes it is possible to assign indirect ^{15}N NMR chemical shifts (Table 1). A general feature involving a shift of the resonances of N1 and N2 atoms of pyrazolone and that of N_{py} of the pyridine ring upon coordination to ruthenium, with the shift of N_{py} being much larger when PTA is present as a coligand.

X-ray Diffraction Study. As stated before, although the structure of the $HL^{py,ph}$ ligand was previously reported,[13] we reobtained its crystal structure to confirm the rotamer I-r

Table 1. ^{15}N Chemical Shifts (ppm) in the Free Ligands and Complexes Obtained from {^{1}H−^{15}N} HMBC NMR Spectroscopy[a]

	N1	N2	N_{py}	N_{PTA}
$HL^{py,ph}$	263.1	194.5	251.9	
1	205.3	157.0	202.9	
2	206.1	n.o.	n.o.	
3	206.8	131.5	176.5	42.5
4	205.6	n.o.	186.5	39.6
$HL^{py,me}$	191.4	322.2	252.4	
5	205.6	135.0	177.1	43.4
6	205.4	139.9	180.4	40.0
$HQ^{py,CF3}$	n.o.	267.9	229.6	
7	n.o.	167.3	179.7	42.8
8	n.o.	172.6	182.8	40.0

[a]n.o. = not observed.

configuration, which is the most stable according to DFT calculations (see below). X-ray data obtained are completely similar to the previous study but with a better R factor (see Table S4). For this reason, no further discussion of the structure of $HL^{py,ph}$ is needed. Complex **3** is crystallized in a monoclinic system with a space group $P2_1/n$, including 8 molecules in the unit cell. In the X-ray structure analysis of **3**, it is noteworthy to mention that there are two independent salts with similar structural parameters and that the crystal shows both enantiomers. One of two crystallographically independent molecules of complex **3** in the asymmetric unit is shown in Figure 1.

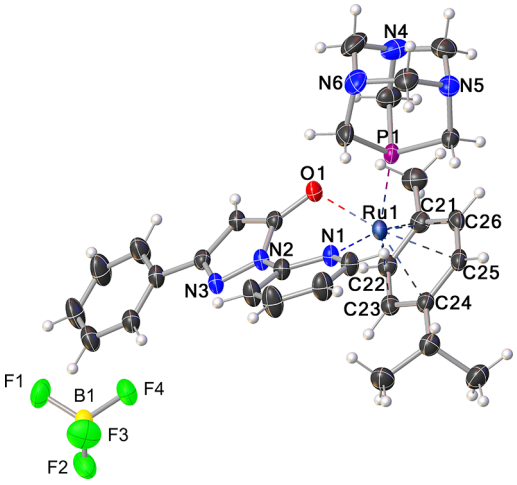

Figure 1. X-ray molecular structure of complex **3** with thermal ellipsoids at the 50% probability level.

Generally, the coordination environment around Ru(II) center possesses octahedral geometry in which the *p*-cymene molecule is bonded in η^6 coordination mode to the metal ion center, while other coordination sites are occupied by deprotonated bidentate L ligand with N7 pyridine atom and deprotonated O2 atom, and P atom of the triaza ligand. Pyrazole ligand bind to the metal center at N and O forming a six-membered chelate ring with bite angles N(7)−Ru(2)−O(2) 83.38(7)° and N(1)−Ru(1)−O(1) 83.10(7)°, bond lengths O(1)−Ru(1) 2.0892(15) and O(2)−Ru(2) 2.0883(15); N(1)−Ru(1) 2.1258(18) and N(7)−Ru(1) 2.1210(18) Å for the complexes. Also, the Ru(II) atom is π-bonded to the arene

https://doi.org/10.1021/acs.organomet.3c00121
Organometallics 2023, 42, 1495−1504

ring with an average Ru(1)−C and Ru(2)−C distance of 1.746 and 1.716 Å respectively. These results show that the complexes have a distorted octahedron structure. Selected bond angles and bond lengths are presented in Table 2.

Table 2. Selected Bond Lengths (Å) and Bond Angles (°) in Complex 3

bond lengths		bond angles	
Ru1−P1	2.3051(6)	O1−Ru1−P1	80.62(4)
Ru1−O1	2.0892(15)	O1−Ru1−N1	83.10(7)
Ru1−N1	2.1258(18)	N1−Ru1−P1	89.95(5)
Ru2−P2	2.3072(6)	N7−Ru2−P2	89.15(5)
Ru2−O2	2.0883(15)	O2−Ru2−P2	78.61(4)
Ru2−N7	2.1210(18)	O2−Ru2−N7	83.38(7)

DFT Study. The possible tautomers and rotamers of the $HL^{py,ph}$ proligand (Chart 2) were examined using density functional theory (DFT) at the B3LYP/6-311+G** level of theory. The resulting optimized structures and their relative energies are collected in Figure S1 (Supporting Information). The most stable form is rotamer I-r, and the theoretical data obtained match well with the experimental behavior of the $HL^{py,ph}$ proligand, both in solution and in the solid state. The calculated NMR spectrum of rotamer I-r correlates well with the experimental spectrum (coefficient of determination, R^2, of 0.9963; see Figure S3) and, additionally, a good fit was found in the comparison of the structural parameters of the calculated $HL^{py,ph}$ molecule with those determined by X-ray crystallography (Figure S2).[13] This confirms the appropriateness of the selected combination of method and basis sets. As previously noted for the related proligand $HL^{py,me}$,[6] the existence in rotamer I-r of an intramolecular hydrogen bond (O−H···N, 1.781 Å; O···N, 2.649 Å; and O−H···N angle of 144.2°) is the key stabilizing factor. Complexes **1**−**4** were also studied by DFT calculations. The selected combination of the method and basis sets provides a good structural description of these complexes based on the comparison of the calculated and experimental structural parameters of complex **3** (Table S1). The resulting optimized structures (Figure 2) show the typical three-legged piano-stool structure, where $L^{py,ph}$ acts as a *N,O* bidentate ligand.

The six-membered $[Ru(L^{py,ph})]$ metallacycle in these complexes displays a half-chair conformation. The angles between the pyrazolone plane and the plane defined by Ru and the N and O donor atoms are around 45° for **1** and **3** (ca. 48° in the X-ray structure) and 41° for **2** and **4**. To rationalize this difference, the structure of the anion $[L^{py,ph}]^-$ was also optimized. Two rotamers with similar energies were located, corresponding to the potential *N,O* or *N,N* bidentate ligands (Figure S4). The deprotonation of rotamer I-r affords a C−O bond of 1.23 Å for the *N,O* rotamer. Upon coordination, this distance increases to approximately 1.29 Å (complexes **1** and **2**) and to around 1.31 Å (**3** and **4**), suggesting a bond order greater than one,[24] and delocalization along the $[Ru(L^{py,ph})]$ metallacycle. These values agree with the observed decrease in the ν_{CO} vibration mode from neutral complexes **1** and **2** to cationic complexes **3** and **4** discussed above. The MOs of $[L^{py,ph}]^-$ involved in the in-plane *N,O* coordination to the ruthenium center are HOMO−1, HOMO−4 and HOMO−6 (Figure 3),

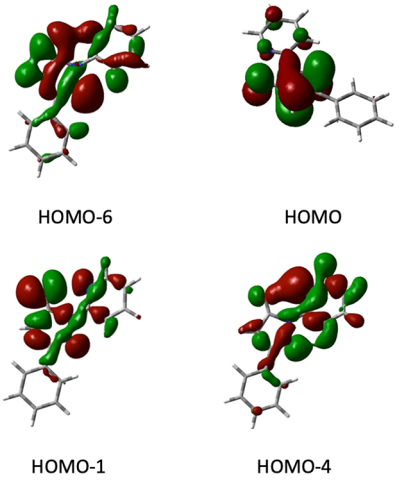

Figure 3. MOs of anionic ligand $[L^{py,ph}]^-$ involved in the *N,O*-coordination to Ru center.

these being MOs in which the lone pairs of the donor N and O atoms participate in the in-phase and out-of-phase contributions of σ type that provide the M−O and M−N bonds in **1**−**4**. However, considering the conformation of the $[Ru(L^{py,ph})]$ metallacycle, some supplementary contribution to the Ru−O bond comes from the π part of the HOMO of the ligand (Figure 3).

Since the $[L^{py,ph}]^-$ ligand also exists as a *N,N* rotamer, the possible ruthenium isomers of **1**−**4** with the *N,N* bidentate ligand were also optimized (Figure S5). Surprisingly, despite the steric hindrance of the Ph substituent, the *N,N* isomers are not clearly destabilized, except for complex **4** (Table S2). This can be explained on the basis of a reinforcement of the Ru-X bonds in the *N,N* isomers that compensates for the steric pressure, which is observed in the calculated Mayer indexes for the Ru−X bonds. An increase in these indexes was observed for the *N,O* complexes compared to the *N,N* isomers (Table S3). On the basis of the similar relative energies shown in Table S2 for complexes **1** and **2** and their isomers, the *N,O* coordination is not clearly favored from a thermodynamic point of view. Therefore, the formation of **1** and **2** is assumed to occur via a mechanism involving nucleophilic attack of the oxygen atom (Mulliken charge of −0.41) on the deprotonated $[L^{py,ph}]^-$ species toward the Ru center. Thus, the only possible bidentate coordination of the ligand involves the formation of the Ru−N bond through the N_{py} atom. For comparison, complexes **5**−**8** were also analyzed by DFT calculations and similar three-legged piano-stool structures were observed in optimized molecules

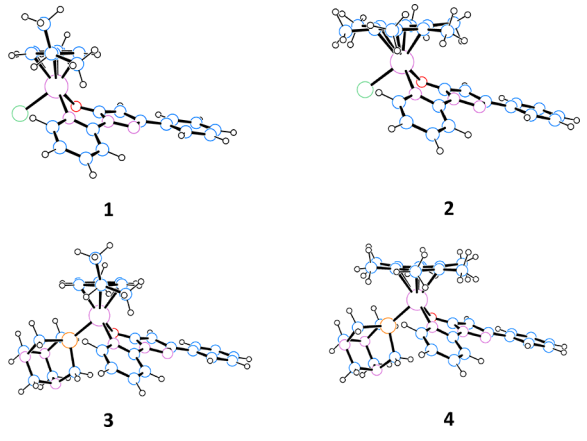

Figure 2. Optimized structures of complexes **1**−**4**.

https://doi.org/10.1021/acs.organomet.3c00121
Organometallics 2023, 42, 1495−1504

(Figure 4). The C−O bond lengths (1.225 Å for **5** and **6** and 1.220 Å for **7** and **8**) are shorter than those observed for

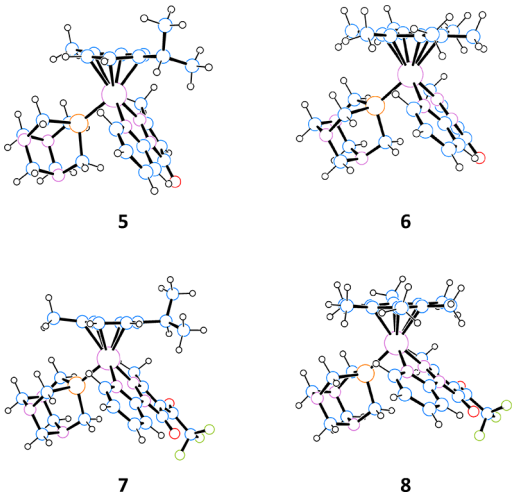

Figure 4. Optimized structures of the cations of complexes **5**−**8**.

complexes **1**−**4** and, consequently, higher ν_{CO} frequencies were observed in agreement with the experimental IR spectra. These complexes are characterized by a HOMO constituted by a d_π ruthenium orbital that displays an antibonding combination with the π part of the L^{py} or $Q^{py,CF3}$ ligands. This situation is similar to that previously reported for the neutral counterparts, [Ru(arene)($L^{py,me}$)Cl] and [Ru(arene)($Q^{py,CF3}$)Cl].[6]

Cytotoxicity Studies. To investigate the stability of **1**−**8** a series of ^{1}H (for the neutral complexes **1**−**2**) and ^{31}P NMR spectra (for the cationic 3−8) were recorded in DMSO-d_6 solution over time (Figures S68−S75). Complexes **1**−**2** undergo partial dissociation of the pyrazolone ligand immediately after dissolution while **3**−**8** are stable in DMSO-d_6 and their ^{31}P NMR spectra remain unchanged within 72 h. Based on these data, we decided to investigate only the cytotoxicity of compounds **3**−**8** against the human ovarian carcinoma cell line (A2780) and its Cisplatin resistant form (A780cis) as well as nontumorigenic human embryonic kidney (HEK293T) cells over an incubation period of 72h using the MTT assay. The resulting IC_{50} values of the compounds are presented in Table 3

Table 3. IC_{50} Values (μM) of the Compounds Tested on Human Ovarian Carcinoma (A2780), Its Cisplatin Resistant Form (A2780cis), and Human Embryonic Kidney Cells (HEK293T)[a]

	A2780	A2780cis	HEK293T
$HL^{py,ph}$	1.7 ± 0.5	1.3 ± 0.4	8 ± 4.4
3	>100	>100	>100
4	>100	>100	>100
$HL^{py,me}$	9.1 ± 1.1	17.4 ± 1.7	14.9 ± 0.1
5	36 ± 19	>100	>100
6	35 ± 7	28 ± 3	33 ± 6
$HQ^{py,CF3}$	8.9 ± 0.5	10.4 ± 2.6	12.9 ± 0.3
7	>100	>100	>100
8	>100	>100	>100
Cisplatin	0.9 ± 0.2	6.7 ± 4	2.2 ± 0.8
Rapta-C	>200	>200	>200

[a]Values are given as the mean obtained from 3 independent experiments ± standard deviation.

together with the values for Cisplatin and Rapta-C used as positive and negative controls, respectively. The proligands are more potent than their corresponding complexes on the ovarian cell line A2780, most notably with $HL^{py,ph}$ with an IC_{50} = 1.7 ± 0.5 μM. It is possible that the active part of the free ligand is the part that coordinates to the metal center and hence it is deactivated unless it is released slowly from the complex after it reaches the cancer cell. In particular, cationic complexes **3** and **4**, resulting from the substitution of the chloride ligand in complexes **1** and **2** by PTA, are essentially inactive (IC_{50} > 100 μM) on the three cell lines. A similar loss of cytotoxicity is observed with complexes **7** and **8** compared to their precursors [Ru(cym)($Q^{py,CF3}$)Cl] and [Ru(hmb)($Q^{py,CF3}$)Cl], respectively. As observed for related Ru(II) half sandwich compounds, the introduction of hydrophilic PTA clearly reduces the lipophilicity of such complexes, which can be disadvantageous to cross cell membranes thus reducing the uptake of complexes in tumor cells.[25]

In contrast, complexes **5** and **6** have a higher potency than [Ru(cym)($L^{py,me}$)Cl] and [Ru(hmb)($L^{py,me}$)Cl] with IC_{50} values of 36 ± 19 and 35 ± 7 μM, respectively. Interestingly, **5** is completely inactive on the nontumorigenic HEK293T cell line (IC_{50} > 100 μM), while being cytotoxic to the ovarian cancer A2780 cell line. Additionally, complex **6** shows similar activity to both A2780 cells and Cisplatin-resistant A2780cis cells (IC_{50} = 35 ± 7 and 28 ± 3 μM, respectively), similar to that observed for related compounds,[26,27] indicating that the mechanism of action is different than Cisplatin.[28−30]

CONCLUSIONS

In this study we have shown that in pyrazolone ligands containing a pyridine ring, the presence of a phenyl in position 3 of the pyrazole ring in $HL^{py,ph}$ in place of a methyl as in $HL^{py,me}$ induces electronic and structural changes that determine the preference for a bidentate *N,O*-coordination, instead of the *N,N*-coordination observed in ruthenium complexes with $HL^{py,me}$. The presence of an acyl moiety in the ligand $HQ^{py,CF3}$ also leads to a preference for an *N,N*-chelated coordination. For complexes **1** and **2** the *N,O* coordination is not clearly thermodynamically favored, according to DFT studies, and their formation maybe occurs via a mechanism involving nucleophilic attack of the oxygen atom in the deprotonated $[Lp^{py,ph}]^-$ ligand toward the Ru center. DFT results rationalize the isolation of $HL^{py,ph}$ as the most stable enol tautomer I in the form of rotamer I-r and describes well the structures of Ru-complexes. These theoretical studies support the spectroscopic assignments (IR and NMR) and, based on the MO analyses of these ligands, provide explanation about their coordination to the Ru center. Anticancer studies performed against A2780, A2780cis, and nontumor HEK293T unexpectedly showed the proligands being more efficient than their corresponding ruthenium complexes. Introduction of a PTA ligand brings the formation of cationic complexes, which are however less active than neutral parents with chloride or completely inactive. In any case, the ligand $HL^{py,ph}$ is quite interesting, being more potent and selective than Cisplatin, and this result may open further developments by exploring the coordination chemistry of such ligand toward other metal acceptors.

EXPERIMENTAL SECTION

Materials and Methods. Solvents were used as supplied or distilled using standard methods. All chemicals were purchased from Aldrich (Milwaukee) and used as received. The dimers [Ru(arene)-

https://doi.org/10.1021/acs.organomet.3c00121
Organometallics 2023, 42, 1495−1504

$Cl_2]_2$ (arene = *p*-cymene (cym) or hexamethylbenzene (hmb)) were purchased from Aldrich. The ligands $HL^{py,me}$ and $HQ^{py,CF3}$ were synthesized by a procedure similar to that previously reported.[6] IR spectra were recorded on a PerkinElmer Frontier FT-IR instrument. ^1H, ^{13}C, ^{31}P NMR spectra were recorded on a 500 Bruker Ascend instrument operating at room temperature relative to TMS. Positive ion electrospray mass spectra were obtained on a Series 1100 MSI detector HP spectrometer, using methanol and acetonitrile as solvent for all complexes **1**−**8**. Solutions (3 mg/mL) for electrospray ionization mass spectrometry (ESI-MS) were prepared using reagent-grade methanol. Masses and intensities were compared to those calculated using IsoPro Isotopic Abundance Simulator, version 2.1.28. Melting points are uncorrected and were recorded on a STMP3 Stuart scientific instrument and on a capillary apparatus. Samples for microanalysis were dried in vacuo to constant weight (20 °C, ca. 0.1 Torr) and analyzed on a Fisons Instruments 1108 CHNS-O elemental analyzer.

X-ray Crystallography. The diffraction data of $HL^{py,ph}$ and **3** were collected, at 140 K, using Cu Kα radiation. Suitable crystals of $HL^{py,ph}$ and **3** were selected and mounted on an XtaLAB Synergy R, DW system, HyPix-Arc 150 diffractometer. The data sets were reduced and corrected for absorption, with the help of a set of faces enclosing the crystals as snugly as possible, with the latest available version of $CrysAlis^{Pro}$.[30]

The solution and refinement of the structures were performed by the latest available version of ShelXT[31] and ShelXL[32] using Olex2−1.5[33,34] as the graphical interface. All non-hydrogen atoms were refined anisotropically using full-matrix least-squares based on $|F|^2$. The hydrogen atoms were placed at calculated positions employing the "riding" model, where each H atom was assigned a fixed isotropic displacement parameter with a value equal to 1.2 U_{eq} of its parent C atom. In $HL^{py,ph}$, the hydrogen atom bound to O1 was found in a difference map and refined freely.

Crystallographic and refinement data for $HL^{py,ph}$ and **3** are summarized in Table S4. The CCDC numbers 2211175 and 2204821 contain the crystallographic data for compounds $HL^{py,ph}$ and **3**, respectively. These data can be obtained free of charge via www.ccdc.cam.ac.uk/data_request/cif.

Computational Details. The electronic structures and geometries of the $HL^{py,ph}$ proligand and the $[L^{py,ph}]^-$ anion, their tautomers, rotamers and ruthenium complexes **1**−**8** and some of their isomers were investigated by using density functional theory at the B3LYP level.[35,36] For the proligand, tautomers, rotamers and its anion the 6-311+G** basis set was used for the optimization, while for Ru compounds the optimization was carried out using LANL2DZ,[37] for the Ru atom and the 6-31G* basis set for the remaining atoms. Molecular geometries were optimized without symmetry restrictions. Frequency calculations were carried out at the same level of theory to identify all the stationary points as minima (zero imaginary frequencies) and to provide the thermal correction to free energies at 298.15 K and 1 atm. The GIAO method was used for the NMR calculations (^1H, ^{13}C, and ^{15}N NMR isotropic shielding tensors), which were carried out at the 6-311+G(2d,p) level of theory. The computed IR spectra were scaled by a factor of 0.96.[38,39] The DFT calculations were executed using the Gaussian 09 program package.[40] The coordinates of all optimized compounds are collected in a separate associated XYZ file attached to the Supporting Information.

Cytotoxicity Tests on A2780, A2780cis, and HEK293T Cell Lines. The human ovarian carcinoma cell line and its Cisplatin resistant form, A2780 and A2780cis, were purchased from the European Collection of Cell Cultures (ECACC, United Kingdom). The human embryonic kidney 293T cell line (HEK293T) was kindly provided by the biological screening facility (EPFL, Switzerland). Fetal bovine serum (FBS) was obtained from Sigma, Switzerland. RPMI 1640 GlutaMAX and DMEM GlutaMAX media were purchased from Life Technologies. The cells were cultured in RPMI 1640 GlutaMAX supplemented for the ovarian cancer cell lines A2780 and A2780cis and in DMEM GlutaMAX supplemented for HEK293T with 10% heat-inactivated FBS at 37 °C and CO_2 (5%). To uphold Cisplatin resistance, the A2780cis cell line was routinely treated with Cisplatin at a final concentration of 2 μM in the media. MTT (3-(4,5-dimethyl-2-thiazolyl)-2,5-diphenyl-2*H*-tetrazolium bromide) assay was used to evaluate the cytotoxicity of the compounds. Stock solutions were prepared in DMSO and sequentially diluted in cell culture grade water to obtain a concentration range of 0−1 mM. Ten μL aliquots of these prepared compound solutions were added in triplicates to a 96-well plate to which 90 μL of the cell suspension (approximately 1.4×10^4 cells/well) were added (final volume 100 μL/concentrations range 0−100 μM). Cisplatin and RAPTA-C were used as positive (0−100 μM) and negative (0−100 μM) controls, respectively, and the plates were incubated for 72 h. Ten microliters of an MTT solution prepared at a concentration of 5 mg/mL in Dulbecco's phosphate buffered saline (DPBS) was added to the cells, and the plates were incubated for additional 4 h. The culture media was carefully aspirated to preserve the purple formazan crystals that were dissolved in DMSO (100 μL/well). The absorbance of the resulting solutions, which is directly proportional to the number of surviving cells, was measured at 590 nm using SpectroMax M5e microplate reader and the data was analyzed with GraphPad Prism software (version 9.3.1). The reported IC_{50} values are based on the means of three independent experiments, each comprising three tests per concentration level.

Synthesis of Proligand $HL^{py,ph}$ and Complexes 1−8. *Proligand $HL^{py,ph}$.* The proligand $HL^{py,ph}$ was synthesized with a different procedure from those reported in the literature,[10−13] which increases its yield. $HL^{py,ph}$ was synthesized by reacting equimolar amounts of 2-hydrazineylpyridine (2.29 g, 21 mmol), and ethyl 3-oxo-3-phenyl-propanoate (4.04 g, 21 mmol) at room temperature. A solution of KOH (87.9%) (100 mg, 1.57 mmol) in methanol (about 20 mL) was added to the mixture. The initial violet mixture was stirred 1 h at room temperature, changing to dark blue. The solution was dried on a rotavapor until an oil was obtained, which was dissolved in hot acetonitrile. The final product crystallized by slow cooling and evaporation (4.52 g, 0.019 mol, yield 90.7%). It is a dark blue solid opaque crystal, highly soluble in alcohols, DMSO, DMF, acetone, acetonitrile, and chlorinate solvents. Anal. Calcd for $C_{14}H_{11}N_3O$ (MW: 237 g/mol): C, 70.87; H, 4.67; N, 17.71%. Found: C, 70.51; H, 4.58; N, 17.83%. mp 121−122 °C. IR (cm^{-1}): 3056w ν(C−H aromatics), 1656m ν(C═O), 1624w ν(C═N), 1596m and 1579m ν(C═C), 1537w, 1489m, 1469s, 1456s, 1441s, 1385m, 1330m, 1296m, 1280m, 999m, 943m, 840m, 814m, 783vs, 749vs, 691s, 655s, 677m, 652m, 590w, 523m, 441s, 407m, 326m, 266w, 194w, 151vs ^1H NMR (500 MHz, $CDCl_3$, 298 K): δ 5.98s (1H, C4−H of $HL^{py,ph}$), 7.17t (1H, $^3J_{(H-H)}$ = 7.5 Hz, C9−H of $HL^{py,ph}$), 7.38t (1H, $^3J_{(H-H)}$ = 7.2 Hz, C14−H of $HL^{py,ph}$), 7.45t (2H, $^3J_{(H-H)}$ = 7.5 Hz, C13,13′-H of $HL^{py,ph}$), 7.90m (3H, C12,12′-H and C8−H of $HL^{py,ph}$), 8.08d (1H, $^3J_{(H-H)}$ = 8.4 Hz, C7−H of $HL^{py,ph}$), 8.30d (1H,, $^3J_{(H-H)}$ = 4.6 Hz, C10−H of $HL^{py,ph}$), 12.84s (1H, OH of $HL^{py,ph}$). ^{13}C NMR ($CDCl_3$, 298 K): δ 8.8 (C4 of $HL^{py,ph}$), 112.3 (C7 of $HL^{py,ph}$), 119.9 (C9 of $HL^{py,ph}$), 125.9 (C13−13′ of $HL^{py,ph}$), 128.6 (C14 of $HL^{py,ph}$), 128.6 (C12−12′ of $HL^{py,ph}$), 133.0 (C11 of $HL^{py,ph}$), 140.0 (C8 of $HL^{py,ph}$), 145.1 (C10 of $HL^{py,ph}$), 152.7 (C3 of $HL^{py,ph}$), 154.5 (C6 of $HL^{py,ph}$), 157.3 (C5 of $HL^{py,ph}$). {$^1H-^{15}N$}-*g*-HMBC NMR ($CDCl_3$, 51 MHz, $^3J_{(N-H)}$ = 3 Hz, 298 K): δ_N 194.5 (N2 of $L^{py,ph}$), 251.9 (N_{py} of $L^{py,ph}$), 263.1 (N1 of $L^{py,ph}$). ESI-MS(−) (CH_3OH) (*m*/*z*, relative intensity%): 236 [100] $[L^{py,ph}]^-$.

*[Ru(cym)($L^{py,ph}$)Cl] (**1**).* $HL^{py,ph}$ (222.7 mg, 0.94 mmol) was dissolved in 20 mL of methanol, KOH (87.9%) was added (65.1 mg, 0.94 mmol) and the mixture was stirred 1 h at room temperature. Then a methanol solution (30 mL) of $[Ru(cym)Cl_2]_2$ (287.8 mg, 0.47 mmol) was slowly added affording a dark green mixture, which was left under stirring at room temperature overnight. The solvent was removed by rotary evaporator, and the crude solid was dissolved in 30 mL of dichloromethane. The mixture was filtered to remove the byproduct KCl, and the volume of filtrate reduced to ca. 4 mL. Then, 30 mL of *n*-hexane were added affording a dark green precipitate, which was filtered off and dried to constant weight (261.4 mg, 0.51 mmol, yield 54.8%). It is soluble in alcohols, DMSO, DMF, acetone, acetonitrile, and chlorinated solvents. Anal. Calcd for $C_{24}H_{24}ClN_3ORu$ (MW: 508 g/mol): C, 56.86; H, 4.77; N, 8.29%. Found: C, 56.59; H, 4.64; N, 8.19%. Λ_m (DMSO, 295 K, 9.8×10^{-4} mol/L): 2.2 S cm^2 mol^{-1}. It decomposes gradually with temperature, starting from about 234 °C. IR (cm^{-1}):

https://doi.org/10.1021/acs.organomet.3c00121
Organometallics 2023, 42, 1495−1504

3419vb (O−H···O, hydrogen bond), 3058w ν(C−H aromatics), 2965w ν(C−H aliphatic), 1635vs ν(C═O), 1483vs and 1461vs δ(C−H), 1370s ν(C−N), 1189w, 1145w, 1091w, 1029w, 940m, 872m, 769vs, 740s, 662s, 520m ν(Ru−N), 450m, 440m ν(Ru−O), 403m, 287vs ν(Ru−Cl), 246vs, 228s, 202m. ^{1}H NMR (500 MHz, CD_3CN, 298 K): δ 0.94d, 0.97d (6H, $^3J_{(H-H)}$ = 6.9 Hz, $CH_3-C_6H_4-CH-(CH_3)_2$ of cym), 2.17s (3H, $CH_3-C_6H_4-CH-(CH_3)_2$ of cym), 2.32hept (1H, $^3J_{(H-H)}$ = 6.9 Hz, $CH_3-C_6H_4-CH-(CH_3)_2$ of cym), 4.76d, 4.88d (2H, $^3J_{(H-H)}$ = 6.0 Hz, $CH_3-C_6H_4-CH-(CH_3)_2$ of cym), 5.14s (1H, C4−H of $L^{py,ph}$), 5.17d, 5.43d (2H, $^3J_{(H-H)}$ = 6.0 Hz, $CH_3-C_6H_4-CH-(CH_3)_2$ of cym), 5.14s (1H, C4−H of $L^{py,ph}$), 7.16ddd (1H, $^3J_{(H-H)}$ = 7.2, 5.8 Hz, $^4J_{(H-H)}$ = 1.3 Hz, C9−H of $L^{py,ph}$), 7.58m (3H, C13,13′,14-H of $L^{py,ph}$), 7.92ddd (1H, $^3J_{(H-H)}$ = 8.7, 7.3 Hz, $^4J_{(H-H)}$ = 1.5 Hz, C8−H of $L^{py,ph}$), 7.99dd (2H, $^3J_{(H-H)}$ = 7.9 Hz, $^4J_{(H-H)}$ = 1.7 Hz, C12,12′-H of $L^{py,ph}$), 8.61dd (1H, $^3J_{(H-H)}$ = 8.5 Hz, $^4J_{(H-H)}$ = 1.3 Hz, C7−H of $L^{py,ph}$), 8.86dd (1H, $^3J_{(H-H)}$ = 5.8 Hz, $^4J_{(H-H)}$ = 1.6 Hz, C10−H of $L^{py,ph}$). $^{13}C\{^1H\}$ NMR (500 MHz, CD_3CN, 298 K): δ 18.0 ((CH_3- $C_6H_4-CH-(CH_3)_2$ of cym), 20.8, 21.4 (($CH_3-C_6H_4-CH-(CH_3)_2$), 81.8, 83.0, 84.3, 84.5 ($CH_3-C_6H_4-CH-(CH_3)_2$ of cym), 88.0 (C4 of $L^{py,ph}$), 101.9, 103.1 ($CH_3-C_6H_4-CH-(CH_3)_2$ of cym), 111.1 (C7 of $L^{py,ph}$), 119.4 (C9 of $L^{py,ph}$), 128.4 (C13,13′ oh $L^{py,ph}$), 129.2 (C14,12,12′ of $L^{py,ph}$), 135.0 (C11 oh $L^{py,ph}$), 140.0 (C8 of $L^{py,ph}$), 150.7 (C6 of $L^{py,ph}$), 152.6 (C10 of $L^{py,ph}$), 161.5 (C3 of $L^{py,ph}$), 165.3 (C5 of $L^{py,ph}$). {^{1}H−^{15}N}-*g*-HMBC NMR (CD_3CN, 51 MHz, $^3J_{(N-H)}$ = 3 Hz, at 298 K): δ_N 157.0 (N2 of L^{py}), 202.9 (N_{py} of L^{py}), 205.3 (N1 of L^{py}). ESI-MS (+) (CH_3CN) (*m*/*z*, relative intensity%): 472 [100] $[Ru(hmb)L^{py,ph}]^+$.

*[Ru(hmb)($L^{py,ph}$)Cl] (**2**).* Complex **2** was prepared using a method similar to that of **1**, using $HL^{py,ph}$ (184.9 mg, 0.78 mmol), KOH (87.9%) (49 mg, 0.78 mmol), and $[Ru(hmb)Cl_2]_2$ (260.7 mg, 0.39 mmol). It was isolated as an orange powder (310 mg, 0.58 mmol, yield 74.3%). It is slightly soluble in alcohols and acetonitrile and soluble in DMSO, DMF, and chlorinated solvents. Anal. Calcd for $C_{26}H_{28}ClN_3ORu$ (MW: 535 g/mol): C, 58.37; H, 5.28; N, 7.85%. Found: C, 58.26; H, 5.27; N, 7.72%. Λ_m (DMSO, 296 K, 8.3 × 10^{-4} mol/L): 2.8 S cm^2 mol^{-1}. It decomposes gradually with temperature starting from about 295 °C. IR (cm^{-1}): 3105w νs(C−H aromatics), 3054w νa(C−H aromatics), 2921w ν(C−H aliphatic), 1633vs ν(C═O), 1593s ν(C═C), 1578m ν(C═N), 1558m, 1485vs and 1405m δ(C−H), 1356s ν(C−N), 1289m, 1235w, 1183w, 1147w, 1087w, 1075w, 1025m, 992m, 762vs, 749s, 676w, 666s, 627m, 529m, 507m ν(Ru−N), 473m, 455m, 439m ν(Ru−O), 401m, 355w, 304s, 291s ν(Ru−Cl), 264m, 227m, 202s. ^{1}H NMR (500 MHz, $CDCl_3$, 298 K) δ, 2.00s (18H, $C_6(CH_3)$ of hmb), 5.86s (1H, C4−H of $L^{py,ph}$), 7.13ddd (1H, $^3J_{(H-H)}$ = 7.3, 5.8 Hz; $^4J_{(H-H)}$ = 1.5 Hz, C9−H of $L^{py,ph}$), 7.37m (1H, C14−H of $L^{py,ph}$), 7.44dd (2H, $^3J_{(H-H)}$ = 8.3, 6.9 Hz, C13,13′-H of $L^{py,ph}$), 7.80ddd (1H, $^3J_{(H-H)}$ = 8.7, 7.1 Hz, $^4J_{(H-H)}$ = 1.8 Hz, C8−H of $L^{py,ph}$), 7.90m (3H, $^3J_{(H-H)}$= 8.3, 1.6 Hz, C12,12′-H of $L^{py,ph}$ and C7−H of $L^{py,ph}$), 8.47dd (1H, $^3J_{(H-H)}$= 5.9 Hz, $^4J_{(H-H)}$ = 1.8 Hz, C10−H of $L^{py,ph}$). ^{13}C NMR (500 MHz, $CDCl_3$, 298 K): δ 15.2 (CH_3 of hmb), 87.2 (C4 of $L^{py,ph}$), 91.4 (C_{arom} of hmb), 115.3 (C7 of $L^{py,ph}$), 119.8 (C9 of $L^{py,ph}$), 125.8 (C12−12′ of $L^{py,ph}$), 128.3 (C14 of $L^{py,ph}$) 128.4 (C13−13′ of $L^{py,ph}$), 133.9 (C11 of $L^{py,ph}$), 139.1 (C8 of $L^{py,ph}$), 150.7 (C6 of $L^{py,ph}$), 152.0 (C10 of $L^{py,ph}$), 155.3 (C3 of $L^{py,ph}$), 163.7 (C5 of $L^{py,ph}$). {^{1}H−^{15}N}-*g*-HMBC NMR ($CDCl_3$, 51 MHz, $^3J_{(N-H)}$ = 3 Hz, 298 K): δ_N 206.1 (N1 of $L^{py,ph}$), N_{py} and N2 of $L^{py,ph}$ not observed. ESI-MS (+) (CH_3CN) (*m*/*z*, relative intensity%): 500 [100] $[Ru(hmb)L^{py,ph}]^+$.

*[Ru(cym)($L^{py,ph}$)PTA]BF_4 (**3**).* Complex **1** (107.5 mg, 0.21 mmol) was dissolved in 30 mL of methanol and 3 mL of an aqueous solution of $AgBF_4$ (41.7 mg, 0.21 mmol) were added. PTA (0.034 mg, 0.21 mmol) was then added, and the mixture stirred 2 h at room temperature. The initial brown-green solution turned to pale green within time. After removal of the byproduct AgCl by filtration, the volume of filtrate was reduced to ca. 4 mL and Et_2O (about 30 mL) was added, with formation of a dark green precipitate, which was identified as complex **3** (101 mg, 0.14 mmol, yield 67%). It is very soluble in alcohols, acetonitrile, DMSO, DMF and acetone, and slightly soluble in water and chlorinated solvents. Anal. Calcd for $C_{30}H_{36}BF_4N_6OPRu$ (MW: 715 g/mol): C, 50.36; H, 5.07; N, 11.75%. Found: C, 50.13; H, 5.17; N, 11.65%. Λ_m (DMSO, 294 K, 9.9.10^{-4} mol/L): 23.4 S cm^2 mol^{-1}. It decomposes gradually with temperature starting from about 235 °C. IR (cm^{-1}): 3074w ν(C−H aromatics), 2924w ν(C−H aliphatic), 1626s ν(C═O), 1483s, 1447s, 1373s. 973s, 947s, 803m, 742s, 698s, 662m, 581vs, 519s, 476s, 451s, 389s, 336m, 305m, 229m, 203m. ^{1}H NMR (500 MHz, CD_3CN, 298 K): δ 0.82d, 0.94d (6H, $^3J_{(H-H)}$ = 6.9 Hz, $CH_3-C_6H_4-CH-(CH_3)_2$ of cym), 2.22s (3H, $CH_3-C_6H_4-CH-(CH_3)_2$), 2.33hept (1H, $^3J_{(H-H)}$ = 6.9 Hz, $CH_3-C_6H_4-CH-(CH_3)_2$ of cym), 4.01m (6H, $(P-CH_2-N)_3$ of PTA phosphine), 4.45s (6H, $(N-CH_2-N)_3$ of PTA phosphine), 4.90d, 5.16d (2H, $^3J_{(H-H)}$ = 6.2 Hz, $CH_3-C_6H_4-CH-(CH_3)_2$ of cym), 5.22s (1H, C4−H of $L^{py,ph}$), 5.69d, 5.72d (2H, $^3J_{(H-H)}$ = 6.2 Hz, $CH_3-C_6H_4-CH-(CH_3)_2$ of cym), 7.25ddd (1H, $^3J_{(H-H)}$ = 7.3, 5.9 Hz, $^4J_{(H-H)}$ = 1.4 Hz, C9−H of $L^{py,ph}$), 7.57m (2H, C13,13′-H of $L^{py,ph}$), 7.64m (1H, C14−H of $L^{py,ph}$), 7.68m (2H, C12,12′-H of $L^{py,ph}$), 8.10ddd (1H, $^3J_{(H-H)}$ = 8.8, 7.2 Hz, $^4J_{(H-H)}$ = 1.6 Hz, C8−H of $L^{py,ph}$), 8.40dd (1H, $^3J_{(H-H)}$ = 6.0, $^4J_{(H-H)}$ = 1.5 Hz, C10−H of $L^{py,ph}$), 8.78dd (1H, $^3J_{(H-H)}$ = 8.7, $^4J_{(H-H)}$ = 1.4 Hz, C7−H of $L^{py,ph}$). ^{13}C NMR (500 Hz, 298 K, CD_3CN): δ 18.7 ($CH_3-C_6H_4-CH-(CH_3)_2$ of cym), 20.4, 21.5 ($CH_3-C_6H_4-CH-(CH_3)_2$ of cym), 30.9 ($CH_3-C_6H_4-CH-(CH_3)_2$ of cym), 50.7d ($^1J_{(P-C)}$ = 13.6 Hz, $(P-CH_2-N)_3$ of PTA phosphine), 72.1 ($^3J_{(P-C)}$ = 7.5 Hz, $(N-CH_2-N)_3$ of PTA phosphine), 86.6, 87.6, 89.5 ($CH_3-C_6H_4-CH-(CH_3)_2$ of cym), 89.8 (C4 of $L^{py,ph}$), 90.6, 103.4 ($CH_3-C_6H_4-CH-(CH_3)_2$ of cym), 112.4 (C7 of $L^{py,ph}$), 120.4 ($CH_3-C_6H_4-CH-(CH_3)_2$ of cym), 121.0 (C9 of $L^{py,ph}$), 128.3 (C13,13′ of $L^{py,ph}$), 129.0 (C12,12′ of $L^{py,ph}$), 129.8 (C14 of $L^{py,ph}$), 133.9 (C11 of cym), 141.5 (C8 of cym), 151.3 (C3 of $L^{py,ph}$), 153.3d ($^1J_{(N-C)}$= 5.6 Hz C10 of $L^{py,ph}$), 164.1 (C6 of $L^{py,ph}$), 165.5 (C5 of $L^{py,ph}$). ^{31}P NMR (500 Hz, 298 K, CD_3CN): δ −37.7. {^{1}H−^{15}N}-*g*-HMBC NMR in (CD_3CN, 51 MHz, $^3J_{(N-H)}$ = 3 Hz, at 298 K): δ_N 42.5 (N_{PTA}), 131.5 (N2 of $L^{py,ph}$), 176.5 (N_{py} of $L^{py,ph}$), 206.8 (N1 of $L^{py,ph}$). ESI-MS (+) (CH_3CN) (*m*/*z*, relative intensity%): 472 [100] $[Ru(cym)L^{py,ph}]^+$, 629 [91] [Ru(cym)($L^{py,ph}$)-PTA]$^+$.

*[Ru(hmb)($L^{py,ph}$)PTA]BF_4 (**4**).* Complex **4** has been synthesized similarly to **3**, using complex **2** (75.4 mg, 0.14 mmol), $AgBF_4$ (98% of purity) (28.8 mg, 0.14 mmol), and PTA (97%) (23.5 mg, 0.14 mmol). It is an orange solid (78.0 mg, 0.10 mmol, yield 72.3%) which is very soluble in alcohols, DMSO, DMF, and acetone and chlorinated solvents and slightly soluble in water and acetonitrile. Anal. Calcd for $C_{32}H_{40}BF_4N_6OPRu$ (MW: 743 g/mol): C, 51.69; H, 5.42; N, 11.30%. Found: C, 51.53; H, 5.37; N, 11.21%. Λ_m (DMSO, 297 K, 1 × 10^{-3} mol/L): 25.9 S cm^2 mol^{-1}. It decomposes gradually with temperature after 249 °C. IR (cm^{-1}): 2920w ν(C−H), 1602w ν(C−N), 1587s ν(C═O), 1576s, 1554s, 1469s, 1447m, 1411m, 1365m, 974vs, 950vs, 944m, 785s, 773s, 684w, 671w, 643w, 609w, 582m, 572m, 557s, 524w, 475m, 453m, 392w, 329m, 203m. ^{1}H NMR (500 Hz, 298 K, CD_3CN): δ 2.16s (18H, CH_3 of hmb), 4.04m (6H, $(P-CH_2-N)_3$ of PTA phosphine), 4.45m (6H, $(N-CH_2-N)_3$ of PTA phosphine), 5.91s (1H, C4−H of $L^{py,ph}$), 7.30ddd (1H, $^3J_{(H-H)}$ = 7.3, 5.9 Hz, $^4J_{(H-H)}$ = 1.7 Hz, C9−H of $L^{py,ph}$), 7.42m (1H, C14−H of $L^{py,ph}$), 7.48m (2H, C13,13′-H of $L^{py,ph}$), 7.90m (2H, C12,12′-H of $L^{py,ph}$), 8.05dd (1H, $^3J_{(H-H)}$ = 7.5 Hz, $^4J_{(H-H)}$ = 1.6 Hz, C7−H of $L^{py,ph}$), 8.10ddd (1H, $^3J_{(H-H)}$ = 8.7, 7.1, $^4J_{(H-H)}$ = 1.6 Hz, C8−H of $L^{py,ph}$), 8.13dd (1H, $^3J_{(H-H)}$ = 6.0 Hz, $^4J_{(H-H)}$ = 1.6 Hz, C10−H of $L^{py,ph}$). ^{13}C NMR (500 Hz, 298 K, CD_3CN): δ 15.3 (CH_3 of hmb), 43.4d ($^1J_{(P-C)}$ = 13.5 Hz, $(P-CH_2-N)_3$ of PTA phosphine), 72.3d ($^3J_{(P-C)}$ = 7 Hz, $(N-CH_2-N)_3$ of PTA phosphine), 88.2 (C4 of $L^{py,ph}$), 99.0 (C_{arom} of hmb), 117.3 (C7 of $L^{py,ph}$), 121.8 (C9 of $L^{py,ph}$), 125.5 (C12,12′ of $L^{py,ph}$), 128.7 (C14,13,13′ of $L^{py,ph}$), 133.4 (C11 of $L^{py,ph}$), 141.4 (C8 of $L^{py,ph}$), 151.1 (C6 of $L^{py,ph}$),153.4 (C10 of $L^{py,ph}$), 154.7 (C3 of $L^{py,ph}$), 162.0 (C5 of $L^{py,ph}$). {^{1}H−^{15}N}-*g*-HMBC NMR in (CD_3CN, 51 MHz, $^3J_{(N-H)}$ = 3 Hz, at 298 K): δ_N 39.6 (N_{PTA}), 186.5 (N_{py} of $L^{py,ph}$), 205.6 (N1 of $L^{py,ph}$), N2 of $L^{py,ph}$ not observed. ESI-MS (+) (CH_3OH) (*m*/*z*, relative intensity%): 657 [100] [Ru(hmb)($L^{py,ph}$)PTA]$^+$.

*[Ru(cym)($L^{py,me}$)PTA]BF_4 (**5**).* Complex **5** was prepared from [Ru(cym)($L^{py,me}$)Cl], previously reported.[6] 82.4 mg (0.15 mmol) of the starting complex were dissolved in 30 mL of methanol and it was added to 1 mL of an aqueous solution of $AgBF_4$ (98% of purity) (29.8 mg, 0.15 mmol). PTA (97% of purity) was added (24.3 mg, 0.15 mmol) and the solution was stirred for 2h. An orange solution appeared. AgCl was formed as byproduct, and it was filtered. The remaining solution

https://doi.org/10.1021/acs.organomet.3c00121
Organometallics 2023, 42, 1495−1504

was dried to about 4 mL and about 30 mL of Et_2O was added, affording a brown precipitate which was shown to be complex **5** (240 mg, 0.37 mmol, yield 75.1%). It is soluble in alcohols, acetonitrile, DMSO, DMF, and water. It is slightly soluble in acetone and chlorinated solvents. Anal. Calcd for $C_{25}H_{34}BF_4N_6OPRu$ (MW: 653.44 g/mol): C, 45.95; H, 5.24; N, 12.86%. Found: C, 45.80; H, 5.28; N, 12.72%. Λ_m (DMSO, 297 K, 1×10^{-3} M): 25.3 S cm^2 mol^{-1}. It decomposes gradually with temperature starting from about 234 °C. IR (cm^{-1}): 3596w, 3077w ν(C−H aromatics), 2930w ν(C−H aliphatic), 1625s ν(C═O), 1594m, 1474s, 1442m, 1418m, 1363m, 1013vs, 972vs, 947vs, 895m, 802m, 777m, 741s, 609s, 573s, 520m, 476m, 451m, 392m, 322w, 278m, 248w, 234w, 214w, 202s. ^{1}H NMR (500 Hz, 298 K, DMSO): δ 0.86d, 0.99 (6H, $^3J_{(H-H)}$ = 6.9 Hz, $CH_3-C_6H_4-CH-(CH_3)_2$ of cym), 2.17s (3H, C−CH_3 of $L^{py,me}$), 2.45s (3H, $CH_3-C_6H_4-CH-(CH_3)_2$ of cym), 2.52m (1H, $CH_3-C_6H_4-CH-(CH_3)_2$ of cym), 3.75m (6H, (P−CH_2−N)$_3$ of PTA phosphine), 4.36m (6H, (N−CH_2−N)$_3$ of PTA phosphine), 4.85s (1H, C4−H of $L^{py,me}$), 6.12d, 6.18d, 6.27d, 6.28d (4H, $^3J_{(H-H)}$ = 6.3 Hz, $CH_3-C_6H_4-CH-(CH_3)_2$ of cym), 7.22t (1H, $^3J_{(H-H)}$ = 6.6 Hz, H9 of $L^{py,me}$), 8.08t (1H, $^3J_{(H-H)}$ = 7.9 Hz, C8−H of $L^{py,me}$), 8.49d (1H $^3J_{(H-H)}$ = 8.6 Hz, C7−H of $L^{py,me}$), 8.56d (1H, $^3J_{(H-H)}$ = 5.9 Hz, C10−H of $L^{py,me}$). ^{13}C{^{1}H} NMR (500 Hz, 298 K, DMSO): δ 17.4 (C3−CH_3 of $L^{py,me}$), 19.5 ($CH_3-C_6H_4-CH-(CH_3)_2$ of cym), 21.7, 22.8 ($CH_3-C_6H_4-CH-(CH_3)_2$ of cym), 31.5 ($CH_3-C_6H_4-CH-(CH_3)_2$ of cym), 51.0d ($^1J_{(P-C)}$ = 14.0 Hz, (P−CH_2−N)$_3$ of PTA phosphine), 72.1d ($^3J_{(P-C)}$ = 7.7 Hz, (N−CH_2−N)$_3$ of PTA phosphine), 88.5 (C4 of $L^{py,me}$), 88.6, 89.1, 89.1, 89.2, 89.6, 89.6 ($CH_3-C_6H_4-CH-(CH_3)_2$ of cym), 111.3 (C7 of $L^{py,me}$), 120.9 (C9 of $L^{py,me}$), 142.0 (C8 of $L^{py,me}$), 151.1 (C3 of $L^{py,me}$), 154.4 (C10 of $L^{py,me}$), 160.6 (C6 of $L^{py,me}$), 165.8 (C5 of $L^{py,me}$). ^{31}P{^{1}H} NMR (500 Hz, 298 K, DMSO): δ −31.78. {^{1}H−^{15}N}-*g*-HMBC NMR (DMSO, 51 MHz, $^3J_{(N-H)}$ = 3 Hz, at 298 K): δ_N 43.4 (N_{PTA}), 135.0 (N2 of $L^{py,me}$), 177.1 (N_{py} of $L^{py,me}$), 205.6 (N1 of $L^{py,me}$). ESI-MS (+) (CH_3OH) (*m*/*z*, relative intensity%): 410 [100] [Ru(cym)($L^{py,me}$)]$^+$, 567 [81] [Ru(cym)($L^{py,me}$)PTA]$^+$.

[Ru(hmb)($L^{py,me}$)PTA]BF_4 ***(6)***. Complex **6** was prepared using a method similar to that of **5** from [Ru(hmb)($L^{py,me}$)Cl], previously reported.[6] 213.7 mg (0.45 mmol) of the starting complex were dissolved in 30 mL of methanol. 89.7 mg (0.45 mmol) of $AgBF_4$ (98% of purity) and 73.2 mg (0.45 mmol) of PTA phosphine (97% of purity) were used, affording a brown precipitate which was shown to be complex **6** (168.9 mg, 0.26 mmol, yield 57.5%). It is soluble in water, alcohols, DMSO, DMF, acetonitrile, and chlorinated solvents. It is slightly soluble in acetone. Anal. Calcd for $C_{27}H_{38}BF_4N_6OPRu$ (MW: 681.49 g/mol): C, 47.59; H, 5.62; N, 12.33%. Found: C, 47.36; H, 5.59; N, 12.20%. Λ_m (DMSO, 297 K, 4.5×10^{-4} M): 13.12 S cm^2 mol^{-1}. It decomposes gradually with temperature starting from about 205 °C. IR (cm^{-1}): 3118w ν(C−H aromatics), 2948w, 2919w, 2871w ν(C−H aliphatic), 1655s ν(C═O), 1603m ν(C−N), 1475s, 1441m, 1420m, 1358s, 1007vs, 972vs, 946vs, 893m, 799m, 779s, 734s, 708m, 670w, 609w, 572m, 519m, 475m, 452m, 392w, 355w, 322w, 277w, 248w, 202m. ^{1}H NMR (500 Hz, 298 K, DMSO): δ 2.11s (18H, CH_3 of hmb), 2.13s (C3−CH_3 of $L^{py,me}$) 3.63dd, 3.79dd (6H, $^2J_{(H-H)}$ = 15.0, $^3J_{(P-H)}$ = 3.6 Hz, (P−CH_2−N)$_3$ of PTA phosphine), 4.34s (6H, (N−CH_2−N) of PTA phosphine), 4.82s (1H, C4−H of $L^{py,me}$), 7.28ddd (1H, $^3J_{(H-H)}$ = 7.4, 6.0, $^4J_{(H-H)}$ = 1.5 Hz, C9−H of $L^{py,me}$), 8.08ddd (1H, $^3J_{(H-H)}$ = 8.7, 7.2, $^4J_{(H-H)}$ = 1.5 Hz, C8−H of $L^{py,me}$), 8.14dd (1H, $^3J_{(H-H)}$ = 6.0, $^4J_{(H-H)}$ = 1.6 Hz, C10−H of $L^{py,me}$), 8.56dd (1H, $^3J_{(H-H)}$= 8.6, 1.4 Hz, C7−H of $L^{py,me}$). ^{13}C{^{1}H} NMR (500 Hz, 298 K, DMSO): δ 16.7 (CH_3 of hmb), 17.5 (C3−CH_3 of $L^{py,me}$), 49.8 ((P−CH_2−N)$_3$ of PTA phosphine), 72.0 ((N−CH_2−N)$_3$ of PTA phosphine), 88.5 (C4 of $L^{py,me}$), 102.3 (Carom of hmb), 110.7 (C10 of $L^{py,me}$), 121.4 (C9 of $L^{py,me}$), 141.7 (C7 of $L^{py,me}$), 151.2 (C6 of $L^{py,me}$), 152.0 (C8 of $L^{py,me}$), 160.9 (C3 of $L^{py,me}$), 166.7 (C5 of $L^{py,me}$). ^{31}P NMR (500 Hz, 298 K, DMSO): δ −38.71. {^{1}H−^{15}N}-*g*-HMBC NMR (DMSO, 51 MHz, $^3J_{(N-H)}$ = 3 Hz, at 298 K): δ_N 40.0 (N_{PTA}), 139.9 (N2 of $L^{py,me}$), 180.4 (N_{py} of $L^{py,me}$), 205.4 (N1 of $L^{py,me}$). ESI-MS (+) (CH_3OH) (*m*/*z*, relative intensity%): 438 [100] [Ru(cym)($L^{py,me}$)]$^+$, 595 [55] [Ru(cym)($L^{py,me}$)PTA]$^+$.

[Ru(cym)($Q^{py,CF3}$)PTA]PF_6 ***(7)***. Complex **7** was prepared using a method similar to that of **6** from [Ru(cym)($Q^{py,CF3}$)Cl], previously reported.[6] 38.3 mg (0.07 mmol) of the starting complex were dissolved in 30 mL of methanol and an aqueous solution (1 mL) of $AgPF_6$ (18.5 mg, 0.07 mmol) was added. Then, 11.5 mg (0.07 mmol) of PTA (97% of purity) was added and the solution was stirred for 2 h. AgCl was formed as byproduct, and it was filtered. The remaining dark yellow solution was dried to about 4 mL and about 30 mL of Et_2O was added, affording a yellow precipitate which was shown to be complex **7** (42.5 mg, 0.05 mmol, yield 75.2%). It is soluble in DMSO, DMF. Anal. Calcd for $C_{27}H_{33}F_9N_6O_2P_2Ru$ (MW: 807.61 g/mol): C, 40.16; H, 4.12; N, 10.41%. Found: C, 40.05; H, 4.24; N, 10.30%. It decomposes gradually with temperature, starting from about 281 °C. Λ_m (DMF, 298 K, 1.7×10^{-4} M): 12.23 S cm^2 mol^{-1}. IR (cm^{-1}): 3081w ν(C−H aromatics), 2932w ν(C−H aliphatic), 1697m, 1682 ν(C═O), 1647vs ν(C−N), 1517m, 1464vs, 1340s, 1256s, 1190m, 1150s, 1054vs, 1011vs, 975m, 949m, 834vs ν(PF_6), 773s, 728s, 685m, 611w, 582s,557vs, 525w, 479m, 453m, 384m, 281w. ^{1}H NMR (500 Hz, DMSO, 298 K): δ 0.77d (3H, $^3J_{(H-H)}$ = 6.8 Hz, $CH_3-C_6H_4-CH-(CH_3)_2$ of cym), 1.02d (3H, $^3J_{(H-H)}$ = 6.8 Hz, $CH_3-C_6H_4-CH-(CH_3)_2$ of cym), 2.46s (3H, $CH_3-C_6H_4-CH-(CH_3)_2$ of cym), 2.46m (1H, $CH_3-C_6H_4-CH-(CH_3)_2$ of cym), 2.54s (3H, C3−CH_3 of $Q^{py,CF3}$) 3.89m (6H, (P−CH_2−N)$_3$ of PTA phosphine), 4.40m (6H, (N−CH_2−N)$_3$ of PTA phosphine), 6.12d, 6.31d, 6.33d 6.44d (4H, $^3J_{(H-H)}$ = 6.4 Hz, $CH_3-C_6H_4-CH-(CH_3)_2$ of cym), 7.37ddd (1H, $^3J_{(H-H)}$ = 7.4, 5.9 Hz, $^4J_{(H-H)}$ = 1.4 Hz, C9−H of $Q^{py,CF3}$), 8.20ddd (1H, $^3J_{(H-H)}$ = 8.6, 7.2 Hz, $^4J_{(H-H)}$ = 1.5 Hz, C8−H of $Q^{py,CF3}$), 8.47dd (1H, $^3J_{(H-H)}$ = 8.6 Hz, $^4J_{(H-H)}$ = 1.4 Hz, C7−H of $Q^{py,CF3}$), 8.63dd (1H, $^3J_{(H-H)}$ = 5.9 Hz, $^4J_{(H-H)}$ = 1.5 Hz, C10−H of $Q^{py,CF3}$). ^{19}F{^{1}H} NMR (500 Hz, DMSO, 298 K): δ −69.4s, −70.9s (PF_6^-), −74.5s (CF_3). ^{31}P{^{1}H} NMR (500 Hz, DMSO, 298 K): δ −32.8 (PTA phosphine). ^{13}C{^{1}H} NMR (500 Hz, DMSO, 298 K): δ 19.1 ($CH_3-C_6H_4-CH-(CH_3)_2$ of cym), 20.0 (C3−CH_3 of $Q^{py,CF3}$), 20.9, 22.9 ($CH_3-C_6H_4-CH-(CH_3)_2$ of cym), 31.3 ($CH_3-C_6H_4-CH-(CH_3)_2$ of cym), 50.5d ($^1J_{(P-C)}$ = 14.0 Hz, (P−CH_2−N)$_3$ of PTA phosphine), 71.8 ($^4J_{(P-C)}$ = 7.8 Hz (N−CH_2−N)$_3$ of PTA phosphine), 88.5, 90.1, 90.4 ($CH_3-C_6H_4-CH-(CH_3)_2$ of cym), 99.7 (C4 of $Q^{py,CF3}$) 102.6 ($CH_3-C_6H_4-CH-(CH_3)_2$ of cym), 111.7 (C7 of $Q^{py,CF3}$), 117.2q ($^1J_{(C-F)}$: 289.9 Hz, (C═O)CF_3 of $Q^{py,CF3}$), 122.2 (C9 of $Q^{py,CF3}$), 122.9 ($CH_3-C_6H_4-CH-(CH_3)_2$ of cym), 142.6 (C8 of $Q^{py,CF3}$), 150.0 (C6 of $Q^{py,CF3}$), 154.4 (C10 of $Q^{py,CF3}$), 161.5 (C5 of $Q^{py,CF3}$), 164.3 (C3 of $Q^{py,CF3}$), 170.7q ($^2J_{(C-F)}$ = 35.9 Hz (C═O)CF_3 of $Q^{py,CF3}$). {^{1}H−^{15}N}-*g*-HMBC NMR (DMSO, 51 MHz, $^3J_{(N-H)}$ = 3 Hz, at 298 K): δ_N 42.8 (N_{PTA}), 167.3 (N2 of $Q^{py,CF3}$), 179.7 (N_{py} of $Q^{py,CF3}$), N1 of $Q^{py,CF3}$ not observed. ESI-MS (+) (CH_3CN) (*m*/*z*, relative intensity%): 663 [100] [Ru(cym)($Q^{py,CF3}$)PTA]$^+$, 506 [29] [Ru(cym)($Q^{py,CF3}$)]$^+$.

[Ru(hmb)($Q^{py,CF3}$)PTA]PF_6 ***(8)***. Complex **8** was prepared using a method similar to that of **7** from [Ru(hmb)($Q^{py,CF3}$)Cl], previously reported.[6] 96.1 mg (0.17 mmol) of the starting complex were dissolved in 30 mL of methanol and an aqueous solution (1 mL) of $AgPF_6$ (43.0 mg, 0.17 mmol) was added. Then, 27.5 mg (0.17 mmol) of PTA (97% of purity) was added and the solution was stirred for 2 h. AgCl was formed as byproduct, and it was filtered. The remaining dark yellow solution was dried to about 4 mL and about 30 mL of Et_2O was added, affording a yellow precipitate which was shown to be complex **8**. It is soluble in DMSO, DMF. Anal. Calcd for $C_{29}H_{37}F_9N_6O_2P_2Ru$ (MW: 835.66 g/mol): C, 41.68; H, 4.46; N, 10.06%. Found: C, 41.55; H, 4.54; N, 9.97%. It decomposes gradually from 292 °C. Λ_m (DMF, 298 K, 2×10^{-4} M): 11.88 S cm^2 mol^{-1}. IR (cm^{-1}): 3081w ν(C−H aromatics), 2935w ν(C−H aliphatic), 1674m, 1652s ν(C−N), 1516w, 1464s, 1341m, 1255m, 1192m, 1156s, 1048s, 1017m, 925s, 834vs ν(PF_6), 784s, 725m, 684w, 608w, 582s, 557vs, 524w, 475m, 453w, 392w, 329m, 278w, 203w. ^{1}H NMR (500 Hz, DMSO, 298 K): δ 2.12s (18H, CH_3 of hmb), 2.49s (3H, C3−CH_3 of $Q^{py,CF3}$) 3.83m (6H, (P−CH_2−N)$_3$ of PTA phosphine), 4.37m (6H, (N−CH_2−N)$_3$ of PTA phosphine), 7.42ddd (1H, $^3J_{(H-H)}$ = 7.4, 5.9, $^4J_{(H-H)}$ = 1.5 Hz, C9−H of $Q^{py,CF3}$), 8.20ddd (1H, $^3J_{(H-H)}$ = 8.7, 7.3, $^4J_{(H-H)}$ = 1.5 Hz, C8−H of $Q^{py,CF3}$), 8.23dd (1H, $^3J_{(H-H)}$ = 6.0 Hz, $^4J_{(H-H)}$ = 1.4 Hz, C10−H of $Q^{py,CF3}$), 8.46dd (1H, $^3J_{(H-H)}$ = 8.7 Hz, $^4J_{(H-H)}$ = 1.3 Hz, C7−H of $Q^{py,CF3}$). ^{19}F{^{1}H} NMR (500 Hz, DMSO, 298 K): δ −69.4s, −70.9s (PF_6^-),

https://doi.org/10.1021/acs.organomet.3c00121
Organometallics 2023, 42, 1495−1504

−74.5s (CF_3). $^{31}P\{^1H\}$ NMR (500 Hz, DMSO, 298 K): δ −40.3 (PTA phosphine). $^{13}C\{^1H\}$ NMR (500 Hz, DMSO, 298 K): δ 16.7 (CH_3 of hmb), 20.7 (C3−CH_3 of $Q^{py,CF3}$), 49.6d ($^1J_{(P-C)}$ = 13.4 Hz, (P−CH_2−N)$_3$ of PTA phosphine), 71.9 ($^4J_{(P-C)}$ = 7.5 Hz (N−CH_2−N)$_3$ of PTA phosphine), 99.9 (C4 of $Q^{py,CF3}$), 103.1 ($C_{aromatics}$ of hmb) 111.5 (C7 of $Q^{py,CF3}$), 117.2q ($^1J_{(C-F)}$ = 290.4 Hz, (C═O)CF_3 of $Q^{py,CF3}$), 122.8 (C9 of $Q^{py,CF3}$), 142.5 (C8 of $Q^{py,CF3}$), 150.1 (C6 of $Q^{py,CF3}$), 152.4 (C10 of $Q^{py,CF3}$), 162.3 (C5 of $Q^{py,CF3}$), 164.8 (C3 of $Q^{py,CF3}$), 170.5q ($^2J_{(C-F)}$ = 35.8 Hz (C═O)CF_3 of $Q^{py,CF3}$). $\{^1H-^{15}N\}$-*g*-HMBC NMR (DMSO, 51 MHz, $^3J_{(N-H)}$ = 3 Hz, at 298 K): δ_N 40.0 (N_{PTA}), 172.6 (N2 of $Q^{py,CF3}$), 182.8 (N^{py} of $Q^{py,CF3}$), N1 of $Q^{py,CF3}$ not observed. ESI-MS (+) (CH_3CN) (*m*/*z*, relative intensity%): 691 [100] [Ru(cym)-($Q^{py,CF3}$)PTA]$^+$.

■ ASSOCIATED CONTENT

Supporting Information

The Supporting Information is available free of charge at https://pubs.acs.org/doi/10.1021/acs.organomet.3c00121.

DFT calculations, figures and XYZ coordinates, crystal data and structure refinement, NMR spectra (PDF)

Structure data (XYZ)

Accession Codes

CCDC 2204821 and 2211175 contain the supplementary crystallographic data for this paper. These data can be obtained free of charge via www.ccdc.cam.ac.uk/data_request/cif, or by emailing data_request@ccdc.cam.ac.uk, or by contacting The Cambridge Crystallographic Data Centre, 12 Union Road, Cambridge CB2 1EZ, UK; fax: +44 1223 336033.

■ AUTHOR INFORMATION

Corresponding Authors

Riccardo Pettinari − *School of Pharmacy, University of Camerino, 62032 Camerino, Macerata, Italy;* orcid.org/0000-0002-6313-4431; Phone: +39 0737402338; Email: riccardo.pettinari@unicam.it

Paul J. Dyson − *Institut des Sciences et Ingénierie Chimiques, Ecole Polytechnique Fédérale de Lausanne (EPFL), 1015 Lausanne, Switzerland;* orcid.org/0000-0003-3117-3249; Email: paul.dyson@epfl.ch

Authors

Lorenzo Pietracci − *School of Science and Technology, University of Camerino, 62032 Camerino, Macerata, Italy*

Alessia Tombesi − *School of Pharmacy, University of Camerino, 62032 Camerino, Macerata, Italy*

Fabio Marchetti − *School of Science and Technology, University of Camerino, 62032 Camerino, Macerata, Italy;* orcid.org/0000-0001-5981-930X

Claudio Pettinari − *School of Pharmacy, University of Camerino, 62032 Camerino, Macerata, Italy;* orcid.org/0000-0002-2547-7206

Agustín Galindo − *Departamento de Química Inorgánica, Facultad de Química, Universidad de Sevilla, 41071 Sevilla, Spain;* orcid.org/0000-0002-2772-9171

Farzaneh Fadaei-Tirani − *Institut des Sciences et Ingénierie Chimiques, Ecole Polytechnique Fédérale de Lausanne (EPFL), 1015 Lausanne, Switzerland;* orcid.org/0000-0002-7515-7593

Mouna Hadiji − *Institut des Sciences et Ingénierie Chimiques, Ecole Polytechnique Fédérale de Lausanne (EPFL), 1015 Lausanne, Switzerland*

Complete contact information is available at: https://pubs.acs.org/10.1021/acs.organomet.3c00121

Notes

The authors declare no competing financial interest.

■ ACKNOWLEDGMENTS

F.M. thanks the University of Camerino and the HP Composites. PhD scholarship of L. Pietracci is financed by Italian Ministry of University and Research; project "Composite Materials Hub of Valle del Tronto, Marche region". A.G. thanks the Centro de Servicios de Informática y Redes de Comunicaciones (CSIRC), Universidad de Granada for providing the computing time.

■ REFERENCES

(1) Cruz, M. P. Edaravone (Radicava): A Novel Neuroprotective Agent for the Treatment of Amyotrophic Lateral Sclerosis. *Pharm. Ther.* **2018**, *43* (1), 25−28.

(2) Faria, J. V.; Vegi, P. F.; Miguita, A. G. C.; dos Santos, M. S.; Boechat, N.; Bernardino, A. M. R. Recently Reported Biological Activities of Pyrazole Compounds. *Bioorg. Med. Chem.* **2017**, *25* (21), 5891−5903.

(3) Pettinari, R.; Marchetti, F.; Di Nicola, C.; Pettinari, C. Half-Sandwich Metal Complexes with Diketone-Like Ligands and Their Anticancer Activity. *Eur. J. Inorg. Chem.* **2018**, *2018*, 3521−3536.

(4) Pettinari, R.; Marchetti, F.; Tombesi, A.; Duan, F.; Zhou, L.; Messori, L.; Giacomelli, C.; Marchetti, L.; Trincavelli, M. L.; Marzo, T.; La Mendola, D.; Balducci, G.; Alessio, E. Ruthenium (II) 1, 4, 7-Trithiacyclononane Complexes of Curcumin and Bisdemethoxycurcumin: Synthesis, Characterization, and Biological Activity. *J. Inorg. Biochem.* **2021**, *218*, 111387.

(5) Garufi, A.; Baldari, S.; Pettinari, R.; Gilardini Montani, M. S.; D'Orazi, V.; Pistritto, G.; Crispini, A.; Giorno, E.; Toietta, G.; Marchetti, F.; Cirone, M.; D'Orazi, G. A Ruthenium (II)-Curcumin Compound Modulates NRF2 Expression Balancing the Cancer Cell Death/Survival Outcome According to P53 Status. *J. Exp. Clin. Cancer Res.* **2020**, *39* (1), 1−15.

(6) Pettinari, R.; Marchetti, F.; Tombesi, A.; Di Nicola, C.; Pettinari, C.; Guo, C.; Zhang, Z.; Galindo, A.; Fadaei-Tirani, F.; Hadiji, M.; Dyson, P. J. Arene-Ruthenium (II) Complexes with Pyrazole-Based Ligands Bearing a Pyridine Moiety: Synthesis, Structure, DFT Calculations, and Cytotoxicity. *Inorg. Chim. Acta* **2021**, *528*, 120610.

(7) Dougan, S. J.; Melchart, M.; Habtemariam, A.; Parsons, S.; Sadler, P. J. Phenylazo-Pyridine and Phenylazo-Pyrazole Chlorido Ruthenium-(II) Arene Complexes: Arene Loss, Aquation, and Cancer Cell Cytotoxicity. *Inorg. Chem.* **2006**, *45* (26), 10882−10894.

(8) Needham, R. J.; Sanchez-Cano, C.; Zhang, X.; Romero-Canelón, I.; Habtemariam, A.; Cooper, M. S.; Meszaros, L.; Clarkson, G. J.; Blower, P. J.; Sadler, P. J. In-Cell Activation of Organo-Osmium (II) Anticancer Complexes. *Angew. Chemie Int. Ed.* **2017**, *56* (4), 1017−1020.

(9) Zhang, X.; Ponte, F.; Borfecchia, E.; Martini, A.; Sanchez-Cano, C.; Sicilia, E.; Sadler, P. J. Glutathione Activation of an Organometallic Half-Sandwich Anticancer Drug Candidate by Ligand Attack. *Chem. Commun.* **2019**, *55* (97), 14602−14605.

(10) Basaif, S. A.; Hassan, M. A.; Gobouri, A. A. AlCl3-Catalyzed Diazocoupling of 1-(Aryl/Hetaryl)-3-Phenyl-1H-Pyrazol-2-in-5-Ones in Aqueous Medium. Synthesis of Hetaryl-Azopyrazolones and Their Application as Disperse Dyes. *Dye. Pigment.* **2007**, *72* (3), 387−391.

(11) Huang, Y.-Y.; Lin, H.-C.; Cheng, K.-M.; Su, W.-N.; Sung, K.-C.; Lin, T.-P.; Huang, J.-J.; Lin, S.-K.; Wong, F. F. Efficient Di-Bromination of 5-Pyrazolones and 5-Hydroxypyrazoles by N-Bromobenzamide. *Tetrahedron* **2009**, *65* (46), 9592−9597.

(12) Cho, J.; Sadu, V. S.; Han, Y.; Bae, Y.; Lee, H.; Lee, K.-I. Structural Requirements of 1-(2-Pyridinyl)-5-Pyrazolones for Disproportionation of Boronic Acids. *Molecules* **2021**, *26* (22), 6814.

(13) McFerrin, C. A.; Hammer, R. P.; Fronczek, F. R.; Watkins, S. F. 3-Phenyl-1-(2-Pyrid-yl)-1H-Pyrazol-5-Ol. *Acta Crystallogr. Sect. E* **2006**, *62* (6), o2518−o2519.

(14) Geary, W. J. The Use of Conductivity Measurements in Organic Solvents for the Characterisation of Coordination Compounds. *Coord. Chem. Rev.* **1971**, *7* (1), 81−122.
(15) Palmucci, J.; Marchetti, F.; Pettinari, R.; Pettinari, C.; Scopelliti, R.; Riedel, T.; Therrien, B.; Galindo, A.; Dyson, P. J. Synthesis, Structure, and Anticancer Activity of Arene-Ruthenium(II) Complexes with Acylpyrazolones Bearing Aliphatic Groups in the Acyl Moiety. *Inorg. Chem.* **2016**, *55* (22), 11770−11781.
(16) Marchetti, F.; Pettinari, R.; Di Nicola, C.; Pettinari, C.; Palmucci, J.; Scopelliti, R.; Riedel, T.; Therrien, B.; Galindo, A.; Dyson, P. J. Synthesis, Characterization and Cytotoxicity of Arene-Ruthenium(II) Complexes with Acylpyrazolones Functionalized with Aromatic Groups in the Acyl Moiety. *Dalt. Trans.* **2018**, *47* (3), 868−878.
(17) Caruso, F.; Monti, E.; Matthews, J.; Rossi, M.; Gariboldi, M. B.; Pettinari, C.; Pettinari, R.; Marchetti, F. Synthesis, Characterization, and Antitumor Activity of Water-Soluble (Arene)Ruthenium(II) Derivatives of 1,3-Dimethyl-4-Acylpyrazolon-5- Ato Ligands. First Example of Ru(Arene)(Ligand) Antitumor Species Involving Simultaneous Ru-N7(Guanine) Bonding and Li. *Inorg. Chem.* **2014**, *53*, 3668−3677.
(18) Pettinari, R.; Pettinari, C.; Marchetti, F.; Skelton, B. W. B. W.; White, A. H. A. H.; Bonfili, L.; Cuccioloni, M.; Mozzicafreddo, M.; Cecarini, V.; Angeletti, M.; Nabissi, M.; Eleuteri, A. M. A. M. Arene-Ruthenium(II) Acylpyrazolonato Complexes: Apoptosis-Promoting Effects on Human Cancer Cells. *J. Med. Chem.* **2014**, *57* (11), 4532−4542.
(19) Rosenthal, M. R. The Myth of the Non-Coordinating Anion. *J. Chem. Educ.* **1973**, *50* (5), 331.
(20) Bennett, M.; Matheson, T. W.; Robertson, G. B.; Smith, A. K.; Tucker, P. A. Highly Fluxional Arene Cyclooctatetraene Complexes of Zerovalent Iron, Ruthenium, and Osmium. Single-Crystal x-Ray Study of (Cyclooctatetraene)(Hexamethylbenzene) Ruthenium (0), Ru (. Eta. 6HMB)(1−4-. Eta.-COT). *Inorg. Chem.* **1980**, *19* (4), 1014−1021.
(21) Pettinari, R.; Marchetti, F.; Di Nicola, C.; Pettinari, C.; Galindo, A.; Petrelli, R.; Cappellacci, L.; Cuccioloni, M.; Bonfili, L.; Eleuteri, A. M.; Guedes Da Silva, M. F. C.; Pombeiro, A. J. L. Ligand Design for *N,O*-or *N,N*-Pyrazolone-Based Hydrazones Ruthenium(II)-Arene Complexes and Investigation of Their Anticancer Activity. *Inorg. Chem.* **2018**, *57*, 14123−14133.
(22) Collong, W.; Kruck, T. Mitteilungen Über Metalltrifluorphosphan-Komplexe, 51. Hexakis (Trifluorphosphan) Vanadium(0)-Synthese, Eigenschaften Und Reaktionen. *Chem. Ber.* **1990**, *123* (8), 1655−1656.
(23) Kruck, T. Trifluorophosphine Complexes of Transition Metals. *Angew. Chemie Int. Ed.* **1967**, *6* (1), 53−67.
(24) Cordero, B.; Gómez, V.; Platero-Prats, A. E.; Revés, M.; Echeverría, J.; Cremades, E.; Barragán, F.; Alvarez, S. Covalent Radii Revisited. *Dalt. Trans.* **2008**, No. 21, 2832−2838.
(25) Tremlett, W. D. J.; Tong, K. K. H.; Steel, T. R.; Movassaghi, S.; Hanif, M.; Jamieson, S. M. F.; Söhnel, T.; Hartinger, C. G. Hydroxyquinoline-Derived Anticancer Organometallics: Introduction of Amphiphilic PTA as an Ancillary Ligand Increases Their Aqueous Solubility. *J. Inorg. Biochem.* **2019**, *199*, 110768.
(26) Nazarov, A. A.; Meier, S. M.; Zava, O.; Nosova, Y. N.; Milaeva, E. R.; Hartinger, C. G.; Dyson, P. J. Protein Ruthenation and DNA Alkylation: Chlorambucil-Functionalized RAPTA Complexes and Their Anticancer Activity. *Dalt. Trans.* **2015**, *44* (8), 3614−3623.
(27) Hildebrandt, J.; Häfner, N.; Kritsch, D.; Görls, H.; Dürst, M.; Runnebaum, I. B.; Weigand, W. Highly Cytotoxic Osmium(II) Compounds and Their Ruthenium(II) Analogues Targeting Ovarian Carcinoma Cell Lines and Evading Cisplatin Resistance Mechanisms. *International Journal of Molecular Sciences.* **2022**, *23*, 4976.
(28) Tremlett, W. D. J.; Goodman, D. M.; Steel, T. R.; Kumar, S.; Wieczorek-Błauż, A.; Walsh, F. P.; Sullivan, M. P.; Hanif, M.; Hartinger, C. G. Design Concepts of Half-Sandwich Organoruthenium Anticancer Agents Based on Bidentate Bioactive Ligands. *Coord. Chem. Rev.* **2021**, *445*, 213950.
(29) Riisom, M.; Eade, L.; Tremlett, W. D. J.; Hartinger, C. G. The Aqueous Stability and Interactions of Organoruthenium Compounds with Serum Proteins, Cell Culture Medium, and Human Serum. *Metallomics* **2022**, *14* (7), mfac043.
(30) Steel, T. R.; Hartinger, C. G. Metalloproteomics for Molecular Target Identification of Protein-Binding Anticancer Metallodrugs. *Metallomics* **2020**, *12* (11), 1627−1636.
(31) *CrysAlisPro Software System*; Rigaku Oxford Diffraction, 2021.
(32) Sheldrick, G. M. SHELXT - Integrated Space-Group and Crystal-Structure Determination. *Acta Crystallogr., Sect. A* **2015**, *71* (1), 3−8.
(33) Sheldrick, G. M. Crystal Structure Refinement with SHELXL. *Acta Crystallogr. Sect. C Struct. Chem.* **2015**, *71* (1), 3−8.
(34) Dolomanov, O. V.; Bourhis, L. J.; Gildea, R. J.; Howard, J. A. K.; Puschmann, H. Olex2: A Complete Structure Solution, Refinement and Analysis Program. *J. Appl. Crystallogr.* **2009**, *42* (2), 339−341.
(35) Becke, A. D. Density-Functional Thermochemistry. III. The Role of Exact Exchange., 98:5648−5652. *J. Chem. Phys.* **1993**, *98*, 5648−5652.
(36) Lee, C.; Yang, W.; Parr, R. G. Development of the Colle-Salvetti Correlation-Energy Formula into a Functional of the Electron Density. *Phys. Rev. B* **1988**, *37* (2), 785−789.
(37) Hay, P. J.; Wadt, W. R. Ab Initio Effective Core Potentials for Molecular Calculations. Potentials for K to Au Including the Outermost Core Orbitals. *J. Chem. Phys.* **1985**, *82* (1), 299−310.
(38) Wong, M. W. Vibrational Frequency Prediction Using Density Functional Theory. *Chem. Phys. Lett.* **1996**, *256* (4−5), 391−399.
(39) Scott, A. P.; Radom, L. Harmonic Vibrational Frequencies: An Evaluation of Hartree- Fock, Møller- Plesset, Quadratic Configuration Interaction, Density Functional Theory, and Semiempirical Scale Factors. *J. Phys. Chem.* **1996**, *100* (41), 16502−16513.
(40) Frisch, M. J.; Trucks, G. W.; Schlegel, H. B.; Scuseria, G. E.; Robb, M. A.; Cheeseman, J. R.; Scalmani, G.; Barone, V.; Petersson, G. A.; Nakatsuji, H.; Li, X.; Caricato, M.; Marenich, A.; Bloino, J.; Janesko, B. G.; Gomperts, R.; Mennucci, B.; Hratchian, H. P.; Ortiz, J. V.; Izmaylov, A. F.; Sonnenberg, J. L.; Williams-Young, D.; Ding, F.; Lipparini, F.; Egidi, F.; Goings, J.; Peng, B.; Petrone, A.; Henderson, T.; Ranasinghe, D.; Zakrzewski, V. G.; Gao, J.; Rega, N.; Zheng, G.; Liang, W.; Hada, M.; Ehara, M.; Toyota, K.; Fukuda, R.; Hasegawa, J.; Ishida, M.; Nakajima, T.; Honda, Y.; Kitao, O.; Nakai, H.; Vreven, T.; Throssell, K.; Montgomery, J. A., Jr.; Peralta, J. E.; Ogliaro, F.; Bearpark, M.; Heyd, J. J.; Brothers, E.; Kudin, K. N.; Staroverov, V. N.; Keith, T.; Kobayashi, R.; Normand, J.; Raghavachari, K.; Rendell, A.; Burant, J. C.; Iyengar, S. S.; Tomasi, J.; Cossi, M.; Millam, J. M.; Klene, M.; Adamo, C.; Cammi, R.; Ochterski, J. W.; Martin, R. L.; Morokuma, K.; Farkas, O.; Foresman, J. B.; Fox, D. J. *Gaussian 09*, Revision B.01; Gaussian, Inc.: Wallingford, CT, 2016.

https://doi.org/10.1021/acs.organomet.3c00121
Organometallics 2023, 42, 1495−1504